

Conversion of ethanol to acetone & other produces using nano-sensor SnO₂ (110): Ab initio DFT

Leila Mahdavian

Department of Chemistry, Doroud Branch, Islamic Azad University, Doroud, Iran; Mahdavian_leila@yahoo.com, Mahdavian@iau-doroud.ac.ir

Received 3 February 2011; revised 18 March 2011; accepted 2 April 2011.

ABSTRACT

The material considered in this study, SnO₂ (110), has a widespread use as gas sensor and oxygen vacancies are known to act as active catalytic sites for the adsorption of small molecules. In the following calculations crystal line SnO₂ nano-crystal have been considered. The grains lattice, which has the rutile structure of the bulk material, includes oxygen vacancies and depositing a gaseous molecule, either ethanol, above an atom on the grain surface, generates the adsorbed system. The conductance has a functional relationship with the structure and the distance molecule of the nano-crystal and its dependence on these quantities parallels the one of the binding energy. The calculations have quantum mechanical detail and are based on a semi-empirical (MNDO method), which is applied to the evaluation of both the electronic structure and of the conductance. We study the structural, total energy, thermodynamic and conductive properties of absorption C₂H₅OH on nano-crystal, which convert to acetaldehyde and acetone.

Keywords: Ethanol; Gas Sensor; SnO₂ (110); Electrical Resistance; Semi-Empirical (MNDO).

1. INTRODUCTION

The products of the ethanol dehydrogenation reaction (C₂H₅OH → H₂ + products) depend upon the ensemble size of SnO₂ [1]. Isolated SnO₂ (110) catalyze only the dehydrogenation to acetaldehyde, whereas multiple Cu ensembles show high yields of ethyl acetate in addition to acetaldehyde for surface. Many reactive gases know metal oxides of gas sensors for their sensitivity but they are also ill famed for their cross-sensitivity. A well recognized way for distinguishing gases is using the fact that different kinds of gases tend to react with different ease at the sensor surface and that these therefore give

rise to differently shaped gas sensitivity/surface temperature characteristics [2]. In fact, the results obtained using the nano-spheres clearly demonstrate only the products of mono atomically dispersed Cu (only acetaldehyde is observed) with an apparently improved efficiency [3]. For this reason, it has become popular to apply temperature modulation techniques to metal oxide gas sensors in which the surface temperature is rapidly scanned through a range of temperatures in which there is a strong variation of the gas sensitivity with surface temperature [4-7].

Accordingly, it is important to understand the role of alcohol vapor in the sensing mechanism. The goal of this work is to improve the detection of surface species of SnO₂ thick film gas sensors under their working conditions using computer calculation, and to correlate the sensor signals with the relative changes of the electrical resistance (Ω). Development of ethanol sensors based on thin film technology offers the advantages of greater sensitivity, shorter response time and lower costs.

The SnO₂(110) are showed in **Figure 1** that primitive tetragonal unit cell of the bulk SnO₂. That is orthorhombic super cell of the slab model. The ethanol reactions on SnO₂ (110) show that basic sites participate in alcohol dehydrogenation and 3-hydroxybutanal condensation steps leading to 3-oxobutanal (aldol) and acetone. Chain growth occurs by condensation reactions involving a metal-base bi-functional aldol-type coupling of alcohols.

Reactions of C₂H₅OH-C₂H₄O mixtures show that direct condensation reactions of ethanol can occur without requiring the intermediate formation of gas phase acetaldehyde [8]. In this work, gas sensors based on SnO₂ nano-crystal were fabricated and we report on the ethanol sensing properties of the sensors at various mechanisms in room temperature.

All the calculations were carried out using Gaussian program package. Density Functional Theory (DFT) calculations interaction between them. The results show a sensitivity enhancement in resistance and capacitance when ethanol is near the surface so converted different

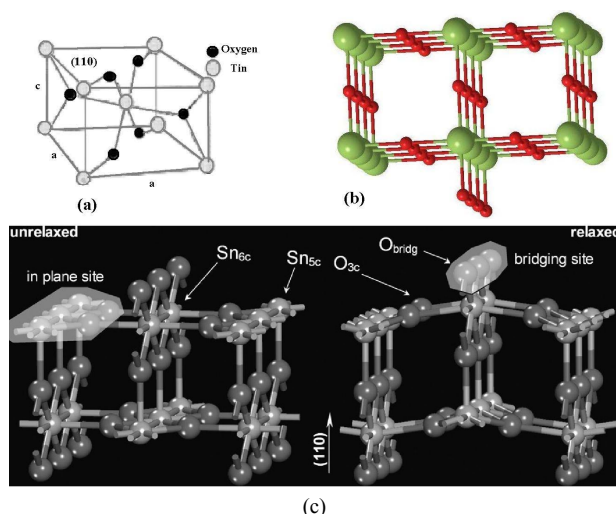


Figure 1. (a) Primitive tetragonal unit cell of the bulk SnO_2 , (b) Optimized configuration Side-view of SnO_2 (110) and (c) the surface adsorption sites for interaction with ethanol.

products.

2. THE COMPUTATIONAL METHODS

The geometry optimizations were performed using an all-electron linear combination of atomic orbital density functional theory (DFT) calculations using the Gaussian program package. In density function theory the exact exchange Hartree-Fock (HF) for a single determinant is replaced by a more general expression the exchange correlation functional which can include terms accounting for both exchange energy and the electron correlation which is omitted from Hartree-Fock theory:

$$E_{KS} = v + \langle hp \rangle + 1/2 \langle P_j(\rho) \rangle + E_{x(\rho)} + E_{c(\rho)} \quad (1)$$

where, $E_{x(\rho)}$ is the exchange function and $E_{c(\rho)}$ is the correlation functional. The correlation function of Lee, Yang and Parr includes both local and nonlocal term. For the Minimum energy structures and cluster size, we employ commercial soft ware from MSI [9] and carry out both linear combinations of atomic orbital (LCAO) and plane wave pseudo potential (PWPP) calculations at the DFT± GGA level. The LCAO basis functions are one-electron orbital of free atoms and free ions [10]. Another advantage is that for specific and well-parameterized molecular systems, these methods can calculate values that are closer to experiment than lower level *ab initio* techniques.

Semi-empirical quantum mechanics method used for calculation all thermodynamic parameters of this interaction. Because, we can use the information obtained from semi-empirical calculations to investigate many thermodynamic and kinetic aspects of chemical processes. Energies and geometries of molecules have clear relationships to chemical phenomena.

The accuracy of semi-empirical quantum mechanics method depends on the database used to parameterize the method. Configuration Interaction (or electron correlation) improves energy calculations using CNDO, INDO, MINDO/3, MNDO, AM1, PM3, ZINDO/1, and ZINDO/S for these electron configurations. The heat of formation is calculated for these methods by subtracting atomic heats of formation from the binding energy. MNDO has been used widely to calculate heats of formation, molecular geometries, dipole moments, ionization energies, electron affinities, and other properties [11, 12]. MNDO gives better results for some classes of molecule, such as some phosphorus compounds.

- Closed-shell singlet ground states
- Half-electron, excited singlet states
- Half-electron, doublet, triplet, and quartet open-shell ground states.

MNDO is a Modified Neglect of Diatomic Overlap method based on the neglect of diatomic differential overlap (NDDO) approximation. In order to compute the average properties from a microscopic description of a real system, one shall evaluate integrals over phase space. It may be calculated for an N -particle system in an ensemble with distribution function $P(r^N)$, the experimental value of a property $A(r^N)$ from:

$$\langle A(r^N) \rangle = \int A(r^N) P(r^N) dr^N \quad (2)$$

The problem with direct evaluation of this multi-dimensional integral (apart of the huge number of phase space points as a sample) is that most of the configurations sampled contribute nothing to the integral. Having energy is so high that the probability of their occurrence is vanishing small [13,14].

The RMS gradient that is reported is just the root-mean square average of the Cartesian components of the gradient vector. For multi-dimensional potential energy surfaces a convenient measure of the gradient vector is the root-mean-square (RMS) gradient described by RMS Gradient:

$$(3N)^{-1} \left[\sum_A \left(\frac{\partial E}{\partial X_A} \right)^2 + \left(\frac{\partial E}{\partial Y_A} \right)^2 + \left(\frac{\partial E}{\partial Z_A} \right)^2 \right]^{1/2} \quad (3)$$

For a molecular mechanics calculation the energy and the gradient are essentially the only quantities available from a single point calculation. Ball-and-stick models of the (110) surface are showed in **Figure 1** that converting of ethanol to other products on SnO_2 (110) simulated by program package and the adsorption, electric, binding nuclear energy, RMS gradient, heat of formation and Gibbs free energy are calculated by MNDO methods in semi empirical quantum by Gaussian program package. The electric resistance for them is following as:

$$E_{elec} = RI \quad (4)$$

where, E_{elec} is electric energy (V), R (Ω) is electric resistance and I (A) is electric intensity that is $I = \frac{q}{t}$ and q (C) is electric charge and t is time interaction, in experimental data, it is so:

$$R = \frac{E_{elec}t}{nF} \quad (5)$$

where, n , F and t are electron number of conversion, faraday constant and time (h) respectively.

3. RESULTS AND DISCUSSION

Therefore, the surface energies of several low-index facets of SnO_2 also known as rutile or tetragonal phase, space group $P4_2mmm$, lattice parameters are $a = b = 4.7374 \text{ \AA}$ and $c = 3.1864 \text{ \AA}$. In the bulk all Sn atoms are six fold coordinated to threefold coordinated oxygen atoms. The surface energies of low index SnO_2 surfaces with a termination that maintains the bulk composition have been calculated (Figure 1) [15-20].

Semi conducting sensors offer an inexpensive and simple method for monitoring gases. The change of the electrical conductivity of semi conducting materials upon exposure to reducing gas $\text{C}_2\text{H}_5\text{OH}$ has been used for gas detection. Therefore, SnO_2 have been used utilizing as the sensing material in pressure, flow, thermal,

gas, optical, mass, position, stress, strain, chemical, and biological sensors [21-23]. Ethanol near SnO_2 surface was converted other products such as: acetaldehyde, ethyl acetate, acetone and etc, which is shown in Figure 2. The mechanism conversion ethanol to other produces on nano-crystal SnO_2 (110) are investigated with MNDO methods. The other methods in DFT can not calculate these parameters for SnO_2 with 24 Sn atoms and theirs calculation are most heavy.

3.1. The Interaction of Ethanol with SnO_2

3.1.1. Formation of Acetaldehyde

It by the oxidative dehydrogenation of ethanol depends critically upon the reaction step that requires the oxide surface to acquire a negative charge. It is well accepted that upon adsorption, the O-H bond of the alcohol dissociates hydrolytically to yield an ethoxide and a proton as follows in Figure 3.

This type of interaction is more known as an acid-base interaction, where the H atom of the acid (in this case ethanol) interacts with one surface O^{2-} (the base). Simultaneously, the Sn^{4+} site (acting as Lewis acid) interacts with the O (2p) orbital of the oxygen of the adsorbed ethanol molecule.

A sequential reaction scheme, where ethanol dehydrogenates to form gas phase acetaldehyde, which then undergoes self-condensation reactions into products, is not considered, because it is not consistent with the

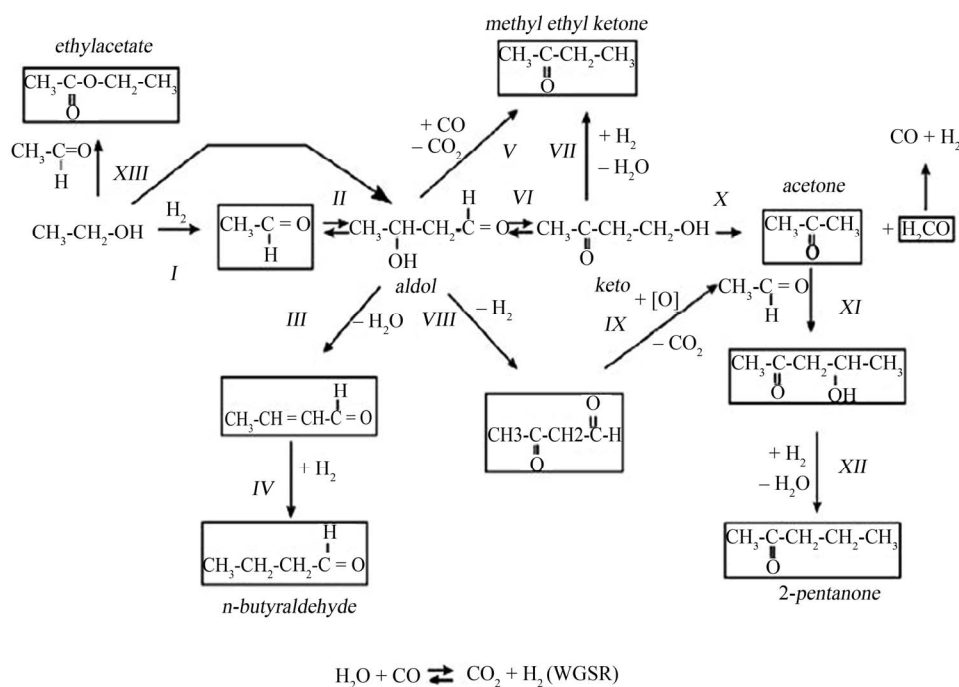


Figure 2. Products of interaction: Ethanol+ SnO_2 .

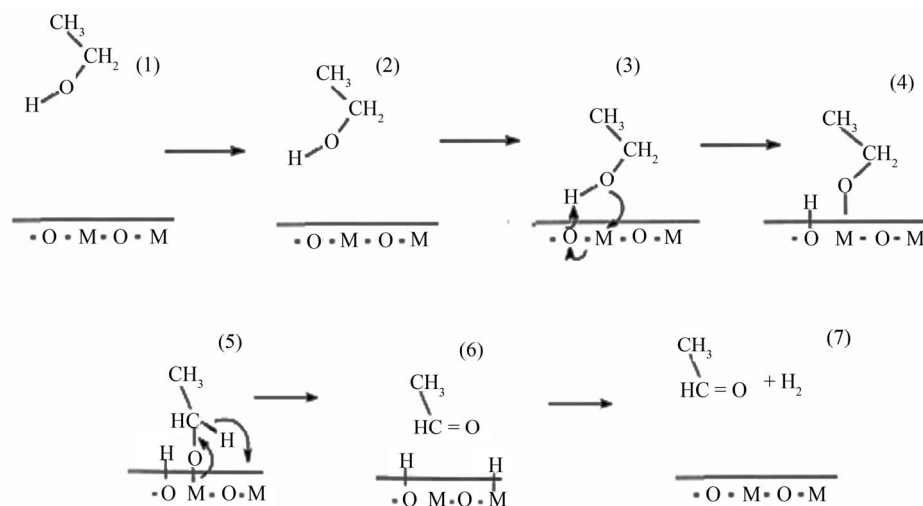


Figure 3. The mechanism converted ethanol to acetaldehyde on SnO₂ (110) by seven steps.

sharp initial increase in product site-yield curves (**Figure 1**). The proposed mechanism involves the initial dissociate adsorption of ethanol on SnO₂ to form ethoxide and hydrogen species. Hydrogen species can then be removed by migration to surface sites, recombination with another hydrogen ad atom, and adsorption as H₂. Additional C–H bond cleavage events in ethoxide species can then occur and the hydrogen atoms formed are transferred to oxygen ions and form surface acetaldehyde species. Ball-and-stick model of this interaction for DFT calculation is seen in **Figure 4**. We calculated that the conductance and thermodynamic properties of this interaction on SnO₂ samples that could be substantially increased or decreased in exposure to ethanol by DFT, which the results are shown in **Table 1**. After adsorption of ethanol on surface and transition electron between them, the electric resistance to time (h) decreased that is shown in **Figure 5**.

A current versus voltage curve recorded with a SnO₂ sample after time exposure to ethanol showed an up-fold of conductance depletion (**Figure 4**). Exposure to ethanol molecules increased the conductance of the SnO₂ sample (**Figure 5**). The SnO₂ is a hole-doped semiconductor, as can be gleaned from the current versus gate voltage curve (middle curve in **Figure 5**), where the electric resistance of the SnO₂ is observed to decrease.

In **Table 1**, the adsorption of energy is negative, which indicates this interaction is exothermic, when ethanol is converted to acetaldehyde; it is -71.13 MJ/mol. Their heat of formation is increased for this conversion on surface because electrons are transferred between surface and ethanol molecule in transient state. The heat of formation is enhanced for intermediates (1433.78 MJ/mol) and transient state (1208.01 MJ/mol) and then it is reduced for product (442.85 MJ/mol). That for binding energy and nucleic energy is too. Suitable default values for ending

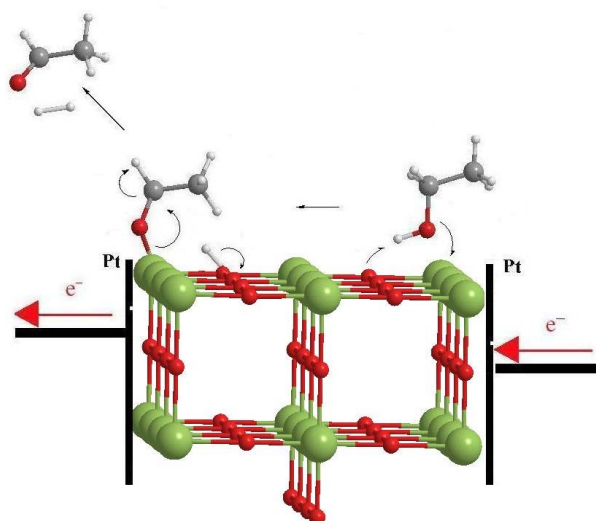


Figure 4. The adsorption ethanol and formation of surface (SnO₂ (110)) ethoxides so converted acetaldehyde.

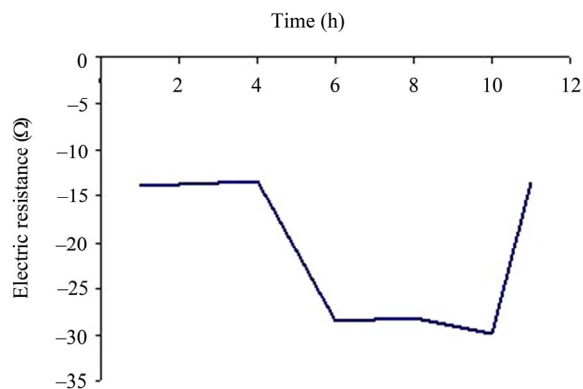


Figure 5. Electrical resistance (Ω) of from Ethanol to acetaldehyde with SnO₂ (100).

Table 1. The properties thermodynamic of interaction ethanol with SnO₂ (110).

<i>Ethanol on SnO₂(110) - based sensor to acetaldehyde</i>				
Time(h)	E _{ads} (MJ/mol)	RMS Kcal/mol.°A	E _{elec} (V)	E _{bin} (MJ/mol)
1	-297.27	1699	-1489.79	963.60
4	-292.09	1357	-1437.89	1433.78
6	-268.30	1546	-1526.91	992.56
8	-71.13	1421	-1507.98	1189.73
10	-83.66	1363	-1601.32	424.57
11	-153.89	1665	-1444.12	1106.97

Time(h)	H (MJ/mol)	G _{ele} (MJ/mol)	E _{nuc} (MJ/mol)
1	981.88	-10142.46	9845.20
4	1452.07	-9789.16	9962.09
6	1010.85	-10395.19	10126.89
8	1208.01	-10266.33	10195.19
10	442.85	-10901.73	10065.43
11	1125.25	-9831.54	9677.64

an optimization calculation are either an RMS gradient of 0.1 Mcal/mol. Å or a maximum number of cycles that is 15 times the number of atoms involved in the calculation. In general, we must use a gradient limit. For improved precision, use a lower gradient limit. For most organic molecules, this will result in an acceptance ratio of about 0.9, which means that about 50% of all moves are accepted. This result shows why surfaces that promote oxidative dehydrogenation reactions tend to be those containing reducible and reoxidisable cations. The residual hydrogen from ethanol adsorption generally desorbs either as H₂.

3.1.2. Formation of Ethyl Acetate

Now, in environment of reaction, there are ethanol and acetaldehyde that ethyl acetate represents the second most important reaction product in our calculations. The intermediates and transient states for this interaction are seen in **Figure 6**. In this reaction requires H transfer from one adsorbed acetaldehyde, which becomes oxidized to another adsorbed ethanol, which is reduced to

alkoxide.

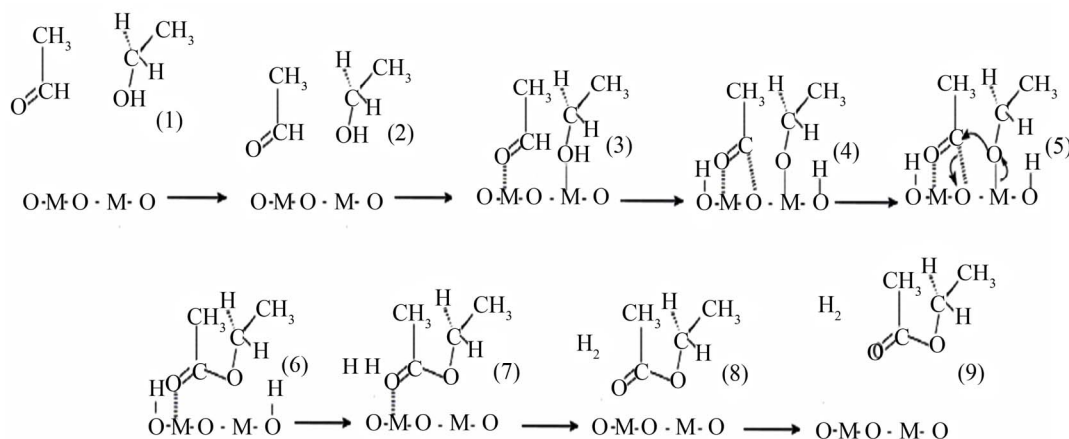
This process may form a complex in a transition state that requires participation of the surface oxygen: where an adsorbed acetaldehyde molecule with the participation of a surface oxygen anion transfers a hydride to another adsorbed ethanol molecule that in **Figure 7** showed ballstick model for it. In this figure is seen ethanol and acetaldehyde near by Sn⁴⁺, so their O atom interacted with Sn⁴⁺ surface. All stapes of this interaction is showed in **Figure 6** by nine steps.

The retention of oxygen associated with the C (5th step in **Figure 6**) intermediate believed to be caused by the strong bonding of the alkyl oxygen in the di-oxygenated CH₃CH₂OCH₃CO⁻ intermediate anion to the ethyl acetate which theirs results showed in **Table 2**. The electric resistance (Ω) for this interaction calculated by **Eq.4** that is showed in **Figure 8**. The ethanol and acetaldehyde are neared to nano-surface and converted to ethyl acetate, their electrons are transferred to SnO₂, and so the electric resistance is decreased.

It is well accepted that upon adsorption, the O–H bond of alcohol and C = O of acetaldehyde dissociates hydrolytically to yield an ethoxide and alkoxide, which intermediate molecules are presented on nano-surface and increased the electric energy (V) in **Table 2**.

It is clear from the table that for all steps the electrical conductivity increased with an increase in the nuclear energy (11355.11MJ/mol) of interaction, indicating the semiconductor enhanced for it in **Figure 8**.

At the same time, the SnO₂ nano-crystal based sensors always showed higher sensitivity to acetaldehyde and ethanol mixture than to ethanol, the adsorption energy is -1269.60 MJ/mol for time 4(h). The hydrogen formation was monitored during steady state ethanol oxidation and SnO₂ were found to be the most active catalysts. These results show that Sn sites also increase rates of C–H bond activation in acetaldehyde and O–H in ethanol. In

**Figure 6.** The mechanism converted ethanol to ethyl acetate on SnO₂ (110) by nine steps.

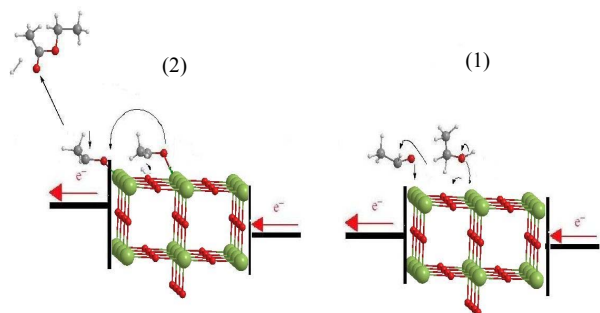


Figure 7. the adsorption ethanol and formation of surface ($\text{SnO}_2(110)$) ethoxides so converted ethyl acetate.

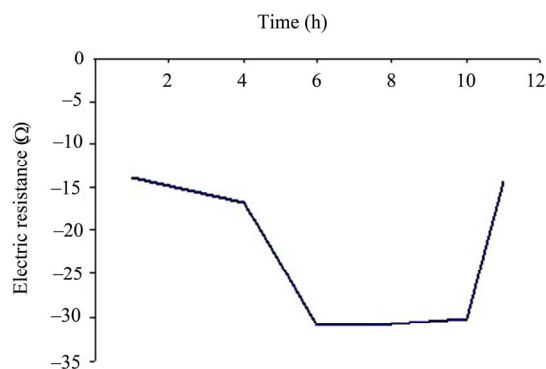


Figure 8. Electrical resistance (Ω) of from ethanol and acetaldehyde to ethyl acetate with $\text{SnO}_2(110)$.

Table.2. The properties thermodynamic of interaction ethanol and acetaldehyde with $\text{SnO}_2(110)$.

<i>Ethanol and acetaldehyde on $\text{SnO}_2(110)$ - based sensor to ethyl acetate</i>				
Time(h)	E_{ads} (MJ/mol)	RMS kcal/mol·Å	E_{elec} (V)	E_{bin} (MJ/mol)
1	-303.03	1484	-1496.14	1622.64
4	-1269.60	1503	-1791.39	1649.98
6	-532.05	1510	-1657.00	1372.81
8	-141.10	1561	-1647.19	1460.70
10	-222.57	1669	-1618.53	1542.18
11	-580.38	1685	-1546.74	1377.64

Time(h)	H (MJ/mol)	G_{ele} (MJ/mol)	E_{nuc} (MJ/mol)
1	1643.48	-10185.68	10488.71
4	1670.82	-12195.73	10926.11
6	1393.65	-11280.83	11334.04
8	1481.54	-11214.02	11355.11
10	1563.02	-11018.90	11241.48
11	1398.49	-10530.17	10588.20

Table 2 is showed, this interaction is exothermic, when they are converted to ethyl acetate; their heat of formation is increased so decreased for this conversion because electrons are translated between surface and so between ethoxide and alkoxide molecules in transient state. The heat of formation has lease amount the intermediates (1393.65 MJ/mol) in time 6 (h) then it is re-

duced to product (1398.46 MJ/mol). The changes of binding energy and nuclear energy are to likes the heat of formation that can see in **Table 2**.

4. CONCLUSIONS

The tin oxide (SnO_2) is a well-known n-type semi conducting oxide that has been widely used for reducing gases in an operating temperature range of 273–443 K. This oxide material has high reactivity towards reducing gases at relatively low operating temperature, easy adsorption of oxygen on its surface because of its natural non-stoichiometry, stable phase and many more desirable attributes such as cheapness and simplicity. For monolayer coverage the C–O bond cleavage process was favored. This appears to be in contradiction to the experimental results discussed above where ethoxide and acetaldehyde production was observed.

At the gas sensor surface, associative adsorption of the ethanol molecules was preferred similar to the DFT calculations. Accurate DFT calculations as well as computationally less expensive interatomic potential based simulations have been employed to study the structures and stabilities of SnO_2 surface and their affinity for ethanol. We investigated the adsorption of ethanol molecules at the under-coordinated (110) surface in SnO_2 . Upon full electronic and geometry optimization, the ethanol molecule associated, with the formation of acetaldehyde on the surface (**Figures 6, 7**), indicating that there is significant energy barrier to the association of an ethanol molecule. The surface energy of a surface is a measurement of its thermodynamic stability, where a low and positive value indicates a stable surface, which showing the interplay between electronic structure calculations and potential-based techniques, is a clear example of the benefits derived in employing complementary methods to identify and investigate important surface features and reactivates.

REFERENCES

- [1] Voort, P.V.D., Baltes, M., Vansant, E.F. and White, M.G. (1997) The uses of polynuclear metal complexes to develop designed dispersions of supported metal oxides: part II. Catalytic Properties. *Interface Science*, **5**, 199-206.
- [2] Moseley, P.T., Norris, J. and Williams, De. Eds. (1991) Techniques and mechanisms in gas sensing. Adam Hilger.
- [3] Gole, J.L. and Whitey, M.G. (2001) Nanocatalysis: selective conversion of ethanol to acetaldehyde using mono-atomically dispersed copper on silica nanospheres. *Journal of Catalysis*, **204**, 249-252.
- [4] Heilig, A., Barsan, N., Weimar, U., Schweizer-Berberich, M., Opel, W.G. and Gardner, J.W. (1997) Gas identification by modulating temperatures of SnO_2 -based

- thick film sensors. *Sensors and Actuators B: Chemical*, **43**, 45-51. doi:10.1016/S0925-4005(97)00096-8
- [5] Jaegle, M., Ollenstein, J.W., Meisinger, T., Böttner, H., Müller, G., Becker, Th. and Braunmühl, C.B.V. (1999) Micromachined thin film gas sensors in temperature pulsed operation mode. *Sensors and Actuators B: Chemical*, **57**, 130-134. doi:10.1016/S0925-4005(99)00074-X
- [6] Faglia, G. (1998) Micromachined gas sensors operated by fast pulsed temperature mode for environmental pollutants. *Proceedings 6th Micro Systems Technologies*, VDE-Verlag, Berlin, pp. S703-S705.
- [7] Hellmich, W., Müller, G., Braunmühl, Ch.B.V., Doll, T. and Eisele, I. (1997) Field effect-induced gas sensitivity changes in metal oxides. *Sensors and Actuators B: Chemical*, **43**, 132-139. doi:10.1016/S0925-4005(97)00195-0
- [8] Idriss, H. (2004) Ethanol Reactions over the Surfaces of Noble Metal/Cerium Oxide Catalysts. *Platinum Metals Rev*, **48**, 105-115. doi:10.1595/147106704X1603
- [9] DMol3 and CASTEP. Molecular Simulations, San Diego. 1998.
- [10] Rantala, T.T., Rantalab, T.S. and Lantto, V. (2000) Electronic structure of SnO₂ (110) surface. *Materials Science in Semiconductor Processing*, **3**, 103-107. doi:10.1016/S1369-8001(00)00021-4
- [11] Gobernado-Mitre, I., Klassen, B., Aroca, R and DeSaja, J. A. (2005) Vibrational spectra and structure of perchlorinated metal-free phthalocyanine and lutetium bisphthalocyanine. *Journal of Raman Spectroscopy*, **24**, 903-908.
- [12] Zverev, V.V., Islamov, R.G., Islamova, F.K. and Vakar, V.M. (1989) Photoelectron spectrum and quantum-chemical structural analysis of N-methyl-N-methoxydiazene-N-oxide. *Journal of Structural Chemistry*, **30**, 228-233.
- [13] Tiana, G., Sutto, L and Broglia, R.A. (2007) Statistical mechanics and its applications. *Physical: A*, **380**, 241-251.
- [14] Mahdavian, L., Monajjemi, M. and Mangkornong, N. (2009) Sensor response to alcohol and chemical mechanism of carbon nanotube gas sensors. *Fullerenes, Nanotubes and Carbon Nanostructures*, **17**, 484-495. doi:10.1080/15363830903130044
- [15] Mangkornong, N., Mahdavian, L., Mollaamin, F. and Monajjemi, M. (2008) Sensing of methanol and ethanol with nano-structured SnO₂ (110) in gas phase: monte carlo simulation. *Journal of Physical and Theoretical Chemistry (IAU.Iran)*, **4**, 197-203.
- [16] Bolzan, A.A., Fong, C., Kennedy, B.J. and Howard, C.J. (1997) Flame spray synthesis of tin dioxide nanoparticles for gas sensing. *Acta Crystallographica Section B: Structural Science*, **53**, 373-380. doi:10.1107/S0108768197001468
- [17] Wang, N., Lin, H., Li, J., Zhang, L., Li, X., Wu, J. and Lin, Ch. (2003) Strong orange luminescence from a novel hexagonal ZnO nanosheet film grown on aluminum substrate by a simple wet-chemical approach. *Journal of the American Ceramic Society*, **90**, 635-637. doi:10.1111/j.1551-2916.2006.01418.x
- [18] Oviedo, J. and Gillan, M.J. (2000) Energetics and structure of stoichiometric SnO₂ surfaces studied by first-principles calculations. *Surface Science*, **463**, 93-101. doi:10.1016/S0039-6028(00)00612-9
- [19] Mulheran, P.A. and Harding, J.H. (1992) The stability of SnO₂ surfaces. *Modelling and Simulation in Materials Science and Engineering*, **1**, 39-43. doi:10.1088/0965-0393/1/1/004
- [20] Slater, B., Catlow, C.R., Gay, D.H., Williams, D.E. and Dusastre, V. (1999) Study of surface segregation of antimony on SnO₂ surfaces by computer simulation techniques. *The Journal of Physical Chemistry B*, **103**, 10644-10650. doi:10.1021/jp9905528
- [21] Li, J., Lu, Y., Ye, Q., Cinke, M., Han, J. and Yyappan, M.Me. (2003) Carbon nanotube sensors for gas and organic vapor detection. *NanoLetters*, **3**, 929-933. doi:10.1021/nl034220x
- [22] Liu, M., Shi, G., Zhang, L., Zhao, G. and Jin, L. (2008) Electrode modified with toluidine blue-doped silica nanoparticles, and its use for enhanced amperometric sensing of hemoglobin. *Analytical Biochemistry*, **391**, 1951-1959.
- [23] Fu, Q. and Liu, J. (2005) integrated single-walled carbon nanotube/microfluidic devices for the study of the sensing mechanism of nanotube sensors. *The Journal of Physical Chemistry B*, **109**, 13406-13408. doi:10.1021/jp0525686